Received: 9 February 2021 | Revised: 14 June 2021 | Accepted: 22 June 2021

DOI: 10.1002/pro.4152

METHODS AND APPLICATIONS

THE PROTEIN SOCIETY WILEY

CyDisCo production of functional recombinant SARS-CoV-2 spike receptor binding domain

Janani Prahlad[1] | Lucas R. Struble[2] | William E. Lutz[2] | Savanna A. Wallin[2] | Surender Khurana[3] | Andy Schnaubelt[1] | Mara J. Broadhurst[1] | Kenneth W. Bayles[1] | Gloria E. O. Borgstahl[2,4]

[1]Department of Pathology and Microbiology, University of Nebraska Medical Center, Omaha, Nebraska, USA

[2]Eppley Institute for Research in Cancer and Allied Diseases, University of Nebraska Medical Center, Omaha, Nebraska, USA

[3]Division of Viral Products, Center for Biologics Evaluation and Research (CBER), FDA, Silver Spring, Maryland, USA

[4]Fred & Pamela Buffett Cancer Center, University of Nebraska Medical Center, Omaha, Nebraska, USA

Correspondence
Gloria E. O. Borgstahl, University of Nebraska Medical Center, 986805 Nebraska Medical Center, Omaha, NE 68198-6805, USA.
Email: gborgstahl@unmc.edu

Funding information
Fred and Pamela Buffett NCI Cancer Center Support Grant, Grant/Award Number: P30CA036727

Abstract

The COVID-19 pandemic caused by SARS-CoV-2 has applied significant pressure on overtaxed healthcare around the world, underscoring the urgent need for rapid diagnosis and treatment. We have developed a bacterial strategy for the expression and purification of a SARS-CoV-2 spike protein receptor binding domain (RBD) that includes the SD1 domain. Bacterial cytoplasm is a reductive environment, which is problematic when the recombinant protein of interest requires complicated folding and/or processing. The use of the CyDisCo system (cytoplasmic disulfide bond formation in *E. coli*) bypasses this issue by pre-expressing a sulfhydryl oxidase and a disulfide isomerase, allowing the recombinant protein to be correctly folded with disulfide bonds for protein integrity and functionality. We show that it is possible to quickly and inexpensively produce an active RBD in bacteria that is capable of recognizing and binding to the ACE2 (angiotensin-converting enzyme) receptor as well as antibodies in COVID-19 patient sera.

KEYWORDS

antigen, COVID19, CyDisCo, protein purification, SARS-CoV-2

1 | INTRODUCTION

The Coronavirus disease-2019 (COVID-19) pandemic caused by the Severe Acute Respiratory Syndrome coronavirus 2 (SARS-CoV-2) has, due to its prolific interhuman transmission, become a dire global health concern.[1] Since its discovery in Wuhan, China[2] in late 2019, there have been over 100 million cases worldwide, and over 2 million deaths as of January 2021. The novel betacoronavirus, SARS-CoV-2, belongs to the *Coronaviridae* family and is closely related to SARS-CoV-1 (79% genomic sequence identity) and MERS-CoV (Middle East respiratory syndrome coronavirus; 50% genomic sequence identity), two other pathogens responsible for the SARS epidemic of 2002, and the MERS epidemic in 2012, respectively.[3,4] SARS-CoV-2 infection elicits a range of clinical presentations, from asymptomatic infection to severe viral pneumonia and death.

Like other coronaviruses, SARS-CoV-2 is comprised of four structural proteins: spike (S), envelope (E), membrane (M), and the nucleocapsid (N).[3,5,6] The S-protein is heavily glycosylated and can be found covering the surface of SARS-CoV-2[7]; glycosylation also allows the virus to evade the host immune system and gain entry into host cells via attachment to its receptor, ACE2.[5,7,8] At the amino acid level, SARS-CoV-2 shares 90% identity with

SARS-CoV-1,[3] yet there are a few distinct structural features between the two variants. The S protein forms a homotrimeric class I fusion protein with each S monomer containing two subunits, S1 and S2.[4,5] When fused to host cell membranes, the S protein undergoes extensive conformational changes that cause dissociation of the S1 subunit from the complex and the formation of a stable postfusion conformation of the S2 subunit. Cell entry is facilitated by two proteases at the cell surface, transmembrane protease serine 2 (TMPRSS2) and cathepsins.[9–11] The S protein of SARS-CoV-2, however, has an additional furin-like cleavage site at the S1/S2 boundary, absent in the SARS-CoV-1 S protein; this cleavage site might enhance viral entry into host cells.

Much like SARS-CoV-1, receptor binding of the SARS-CoV-2 S protein relies on the receptor binding domain (RBD), which recognizes the aminopeptidase N segment of ACE2.[7] In addition to ACE2 recognition, the RBD is also responsible for eliciting neutralizing antibodies (nAbs) and has become a highly investigated target for vaccine and drug development.[3,5,6] Several groups have structurally characterized the SARS-CoV-2 RBD, highlighting important regions and recognition sites for both ACE2 binding, as well as attachment to nAbs. Two independently reported CryoEM structures[5,10] capture the S trimer in the prefusion complex and show that the RBD is capable of a "hinge" movement that either display it ("up") or obscure it ("lying down"). This feature, while damping ACE2 recognition, is thought helpful in immune evasion. Crystal structures of the RBD-ACE2 complex elucidate the interacting regions of the spike RBD and ACE2 complex and highlight the receptor-binding motif (RBM) within the RBD, which makes most of the contacts with ACE2.[4,12] The RBD consists of extensive β-sheets and nine cysteines (Figure 1) which stabilize the overall structure through the formation of four disulfide bonds: three within the β-sheet core (C336–C361, C379–C432, and C391–C525), and one connecting the distal loops of the RBM (C480–C488).

Given the extent of structural similarity (~77%) between SARS-CoV-1 and SARS-CoV-2 RBDs,[11] it is likely that cross-reactive antibodies might exist. Initial studies exploring cross-reactivity of SARS-CoV-2 RBD with mAbs (murine monoclonal antibodies) known to bind SARS-CoV RBD demonstrated little-to-no cross-reactivity.[5,7,13] Despite the high degree of conservation in the S2 subunit,[10] SARS-CoV-1-based monoclonal antibodies have not demonstrated appreciable binding to SARS-CoV-2 RBD,[4] except for CR3022, which bears further study. We note that in earlier constructs the disulfide partner of Cys538 was omitted from the construct and this lead to disorder in the expressed RBD. The construct of RBD used in this article (Figure 2a,b) was designed by studying the first cryoEM structure of SARS-CoV-2

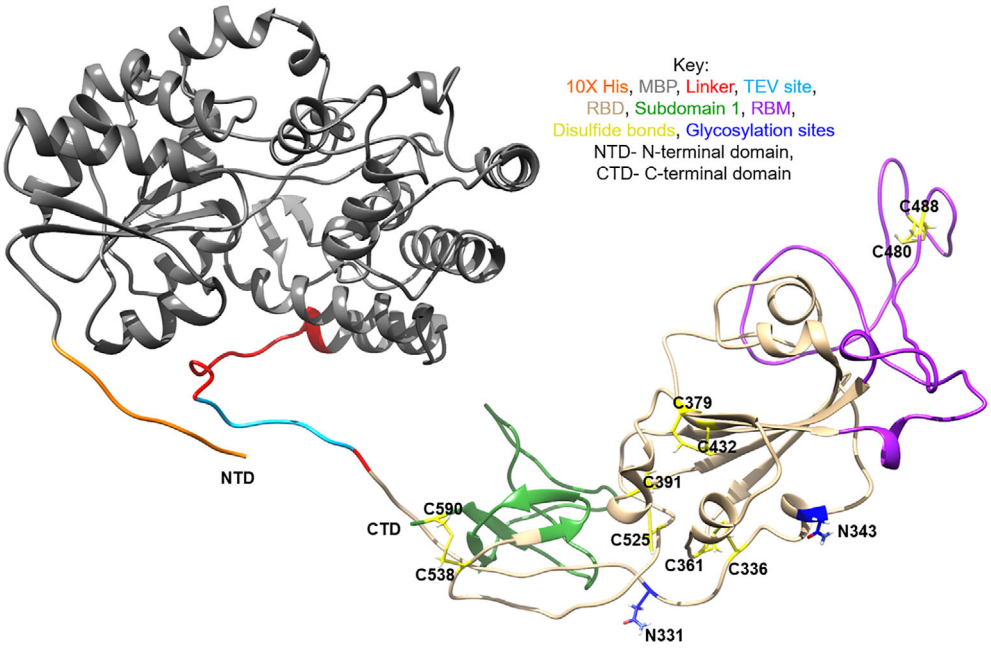

FIGURE 1 Ribbon diagram of MBP fused to SARS-CoV-2 spike RBD showing intramolecular disulfide bonds in yellow. As the structures solved for the RBD had missing gaps in the loops, we fed our sequence into I-Tasser, which generated the complete model of the fusion protein.[14–16] The ribbon was drawn and colored using UCSF Chimera.[27] MBP is depicted in grey, with the linker sequence in light blue and the TEV site in red, followed by the 10× His tag in orange. The RBD is shown colored in tan, with the RBM motif in purple and S1 domain in green. Glycosylated residues are colored blue and disulfide bonds are shown colored yellow

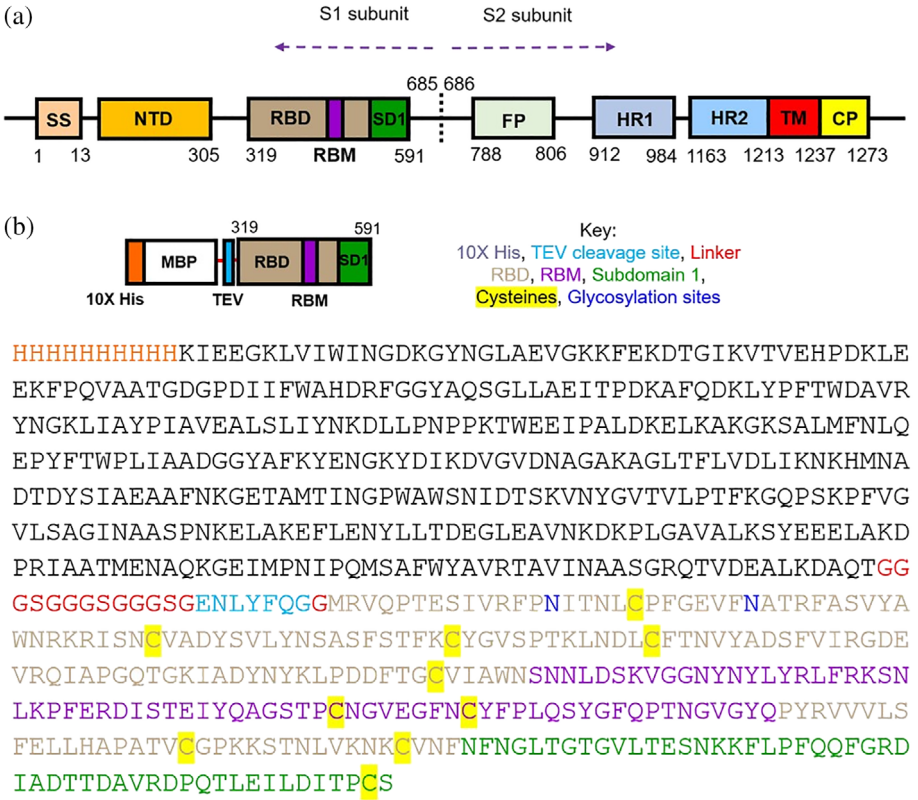

FIGURE 2 (a) Schematic of full-length Spike protein. CP: cytoplasmic peptide; FP: fusion peptide; HR1, HR2: heptad repeats 1 and 2; NTD: N-terminal domain; RBD: Ribosome-binding domain; SS: signal sequence; TM: transmembrane domain. (b) Amino acid sequence of the RBD-MBP fusion protein used in this study. Domains are colored as follows: ×10 His (orange), MBP (white), RBD (tan), RBM (purple), and S1 (green); short linker sequences are shown in red, and the TEV cleavage site is in light blue. Two sites of N-linked glycosylation are colored blue

Spike,[5] the locations of Cys disulfide bonds, and ended the construct to include Cys590. I-Tasser was used to model missing loop regions in the cryoEM structure[14–16] for this fragment and shows that the unsatisfied Cys538 is now expected to form a disulfide with Cys590 of the S1 domain (Figure 1). It is important to note that not all of these disulfide bonds are consecutively formed, some require editing by reduction and reoxidation to form the correct bonds, and this poses a complicated folding problem in the cytoplasm of bacteria.[5]

Both SARS-CoV-2 S protein and its receptor, ACE2, are heavily glycosylated at both N- and O-sites, which can influence viral attachment and entry.[17,18] Several groups have used diverse, sophisticated techniques to probe the effect of glycosylation on viral attachment and immune evasion. The methods used include atomistic molecular dynamics,[3,19] antigenic screens and cryo-EM structure methods,[20] site-specific mass spectrometry,[17] and genetic CRISPR-Cas9 glycoengineering approaches.[21] Their findings reiterate the importance of glycans in viral binding to host ACE2, possibly by steric masking of epitopes,[19,21] as well as influencing the switch of RBD between the "up" and "down" confirmations.[20] Interestingly, Mehdipour and Hummer were able to show that two specific glycosylation mutations in ACE2 (Asn90 and Asn322) resulted in opposite effects where viral binding is prevented or greatly enhanced, respectively.[3] A recent publication by Zhang et al.[22] used a thorough glycoproteomic approach to analyze the diversity of N-glycosylation sequons and N-glycan site occupancy. The authors conclude that the two N-glycosites in the RBD, N331 and N343, are not close enough to directly interact with the ACE2 receptor. Our construct, expressed in bacteria as a fusion protein with MBP, is not glycosylated at Asn331 and Asn343. It is possible that there may be some occlusion of these residues by certain orientations of MBP, but as seen in the model generated through I-Tasser[14–16] and rendered using Chimera[23] in Figure 1, the RBM remains unobstructed and able to interact with ACE2.

Although advantageous in terms of ease of protein production, rapid growth, and cost-efficacy, the production of recombinant proteins in *E. coli* has its challenges. It is vital to maintain the correct disulfide bonds for structural as well as functional stability, which is problematic when expressing proteins of interest in the cytoplasm of wild-type *E. coli*.[24–26] Disulfide bonds are typically formed in proteins that are secreted, or targeted to the outer membrane. The cellular organelles that evolved to carry out this posttranslational modification are the mitochondria and endoplasmic reticulum of eukaryotes, and the periplasmic space in prokaryotes.[26] Disulfide bonds formed in the cytoplasm would be quickly reduced by multiple reductases and/or by reductants (such as glutaredoxin and thioredoxin). A possible solution would be to modify the protein construct to allow its secretion into the periplasm, which contains disulfide bond-catalyzing enzymes.[24,26] However, this

route greatly lessens the protein yield due to the limited cellular space occupied by the periplasm (8–16%) and requires modification of the construct to include a signal sequence for periplasmic targeting.[24] Commercially available strains have been engineered to lack thioredoxin reductase and glutathione reductases, and to express disulfide bond isomerases, such as SHuffle (NEB), and Origami (Novagen), though these strains can suffer from low protein solubility and yield due to the lack of de novo or inappropriate disulfide bond formation.[26]

To circumvent the drawbacks listed above, the Ruddock lab developed the CyDisCo (cytoplasmic disulfide bond formation in *E. coli*) system and showed that it was possible to produce active disulfide-bonded proteins in the cytoplasm of *E. coli* without deleting reduction systems, simply by expressing the sulfhydryl oxidase Evr1p.[26,27] Evr1p uses molecular oxygen to form disulfides in a FAD-dependent reaction, allowing the production of disulfide-bonded proteins in the cytoplasm of wild-type *E. coli*. Another enzyme, protein disulfide isomerase (PDI), is added to edit disulfide bonds during protein folding.[28] PDI can distinguish between properly folded and misfolded proteins, and correct disulfide bonds through cycles of cleavage and formation. In this way, correctly folded proteins with disulfide bonds can be recombinantly produced in the cytoplasm of *E. coli*.

We used the CyDisCo to make recombinant, well-folded, active SARS-CoV-2 spike RBD. By cotransforming the spike RBD expression plasmid with the CyDisCo system plasmid, we were able to successfully produce recombinant spike RBD with disulfide bonds. Here, we describe a simple cost-effective method of generating antigens using a bacterial expression system. By co-expressing our protein of interest along with the CyDisCo system, we have been able to produce folded RBD antigen that retains activity and which can be used in diagnostic assays.

2 | RESULTS AND DISCUSSION

2.1 | Purification of spike RBD-MBP fusion protein

The gene sequence for the Spike RBD-MBP fusion protein was cloned into pET28a and codon-optimized by Genscript. A TEV recognition sequence was included after the MBP protein sequence (Figure 2b) in case cleavage of MBP from RBD was needed. The plasmid containing spike RBD-MBP was co-transformed with the CyDisCo plasmid into BL21(DE3) cells under double antibiotic selection (Figure 3). Initial IPTG induction tests showed appreciable accumulation of the RBD-MBP fusion protein after 16–18 h at 18°C (Figure 4a). Though induction appeared similar to 4-h induction at 30°C, it was decided that lower-temperature induction for a longer time would encourage thorough editing and formation of disulfide bonds and correct folding of the recombinant protein. The cell pellets were lysed with an Emulsiflex, in the presence of protease inhibitor and all subsequent purification steps were performed on ice or at 4°C. After the lysate was clarified by centrifugation, it was passed through a 5 ml MBPTrap affinity column to clear nonspecific proteins lacking the MBP tag. Fractions containing RBD-MBP were confirmed through SDS-PAGE (Figure 4b) where RBD-MBP can be observed running at ~74 kDa (indicated by a black arrow). Interestingly, we could also see prominent bands at ~42 kDa corresponding to the size of MBP, indicating that we may have pulled down a mixture of both endogenously and recombinantly produced *E. coli* MBP. The resulting fractions were pooled before passing through a 1 ml NiAff Nickel affinity column, which bound the ×10 His tag on the fusion protein. This additional affinity purification step helped reduce the amount of nonspecific proteins that co-purify with RBD-MBP, as well as reduce the

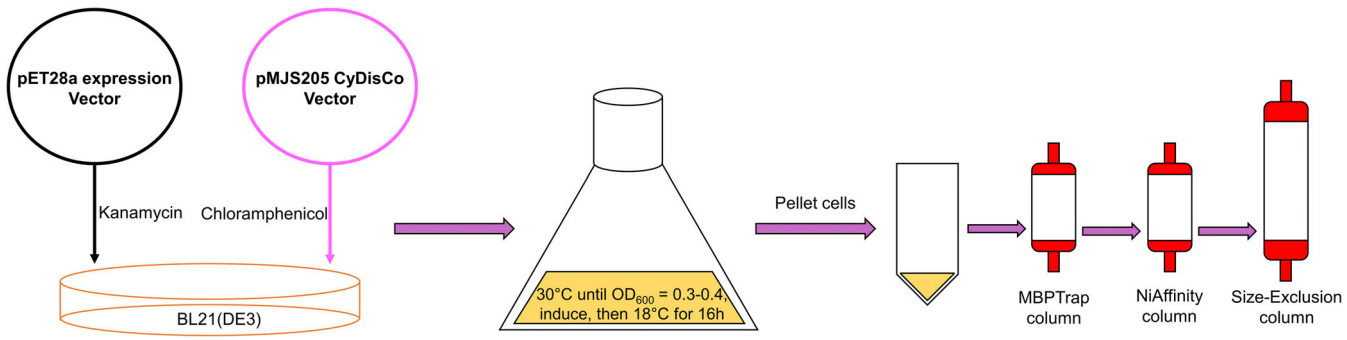

FIGURE 3 Experimental design for RBD-MBP expression and purification. RBD-MBP was cloned into pET28a and co-expressed with CyDisCo vector pMJS205 under kanamycin and chloramphenicol selection. A single colony of BL21(DE3) was inoculated into a few ml of media under antibiotic selection and scaled up into large 2 L flasks. Cells were grown at 30°C until the OD600 reached 0.3–0.4, at which point the cells were induced with 0.5 mM IPTG. The cells expressed protein overnight at 18°C and pelleted the following day. The cell pellet was lysed as described in the main text and passed through three chromatography columns to ensure optimal purity

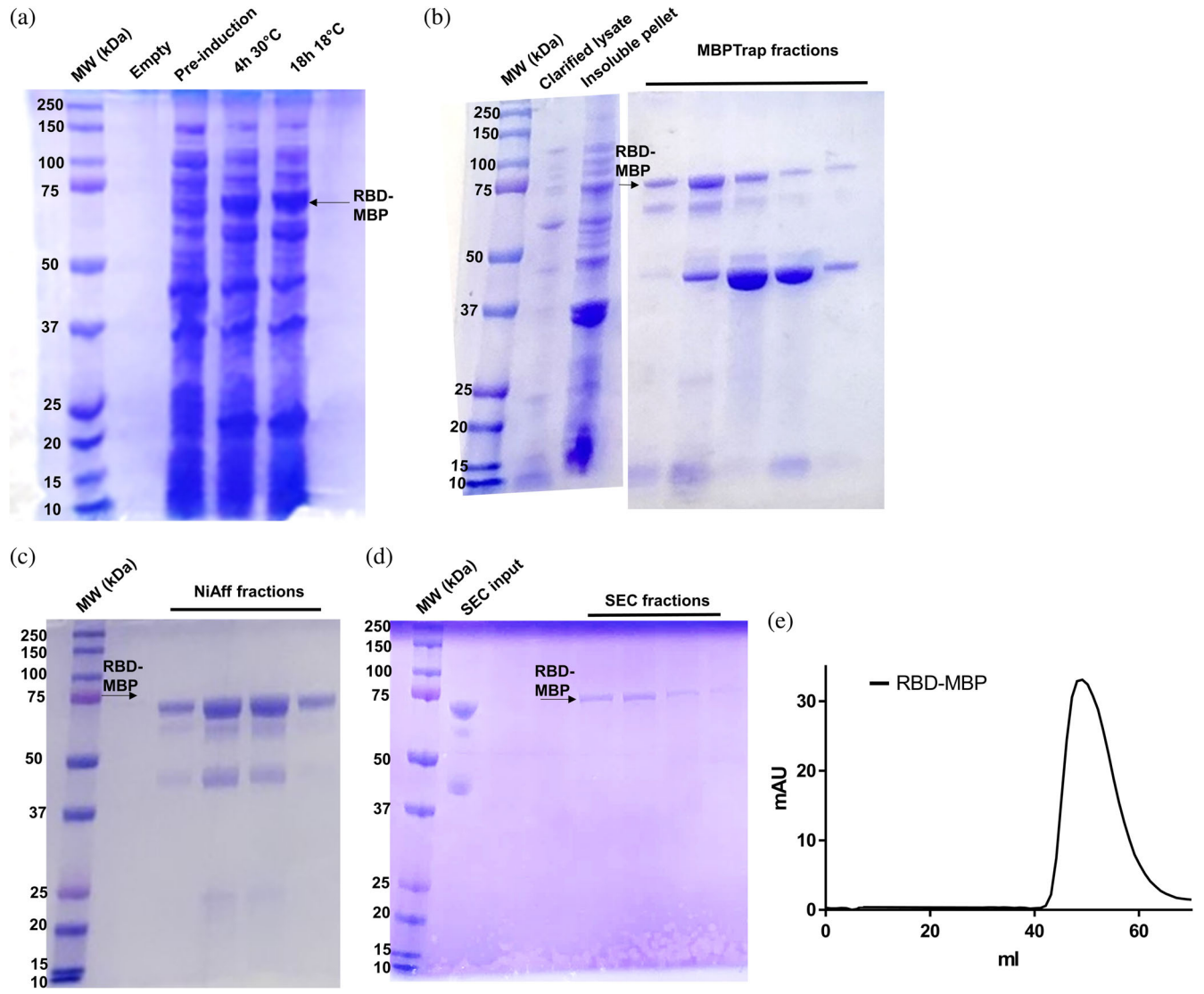

FIGURE 4 Protein purification SDS-PAGE gels. RBD-MBP can be observed running at 74 kDa, as indicated by the black arrows near the 75 kDa marker. (a) Initial induction experiment comparing same-day (4 h) induction at 30°C and overnight (16 h) induction at 18°C. (b) MBPTrap AKTA fractions. (c) Nickel-affinity AKTA fractions. (d) Size-exclusion AKTA fractions. (e) Size-exclusion AKTA chromatogram

presence of any cleaved or endogenous MBP from the pool of fusion protein (Figure 4c). Finally, RBD-MBP was further purified using a size-exclusion step over a Superdex75 column (Figure 4d,e). Using the steps outlined above, without optimization, we were able to obtain approximately 0.25 mg of pure RBD-MBP from 1 L of culture.

2.2 | Binding of spike RBD-MBP to hACE2 receptor

To test the activity of purified RBD-MBP, we assessed its binding to hACE2 using SPR against control RBD made in insect cells (Figure 5a). We showed that the purified RBD-MBP bound hACE2, indicating correct functional folding of the purified recombinant protein.

2.3 | SARS-CoV-2 antibodies in patient serum samples bind to spike RBD-MBP

An immunoassay was performed to confirm that our RBD-MBP was recognized by human SARS-CoV-2-specific antibodies. RBD-MBP-bound microspheres were incubated with sera that had tested positive ($n = 6$) or negative ($n = 6$) in a Luminex-based clinical SARS-CoV-2 serology assay. RBD-specific IgG antibodies were detected in all sera from SARS-CoV-2 antibody-positive patients (Figure 5b).

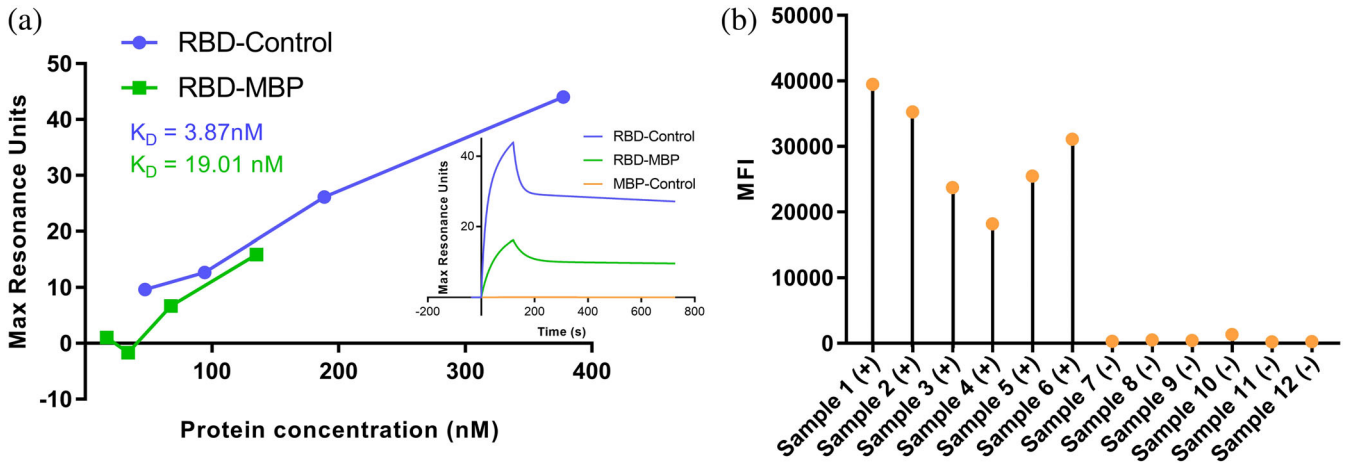

FIGURE 5 Activity assessment of purified recombinant RBD-MBP. (a) SPR binding assay of RBD-MBP to hACE2. Insert contains the sensorgram for the 10 μg/ml concentration data. (b) Microsphere immunoassay of RBD-MBP binding to IgG antibodies in patient sera [(+) = SARS-CoV-2 IgG positive, (−) = SARS-CoV-2 IgG negative]. MFI, mean fluorescence intensity

3 | CONCLUSIONS

In this article, we have described a rapid method to express and purify functionally active SARS-CoV-2 Spike RBD antigen in *E. coli*. The SARS-CoV-2 Spike RBD antigen purified here was designed in-house based on the first cryoEM structure when it was deposited in the protein data bank in February 2020.[5] Unlike earlier RBD expression systems, the RBD domain purified here includes the C-terminal SD1 domain so that all five disulfide bonds are satisfied and the protein fold is stabilized. Through the co-expression of the sulfhydryl oxidase Evr1p, and the disulfide bond isomerase PDI, in the CyDisCo system along with the RBD-MBP plasmid, we have produced well-folded and functionally active protein in a bacterial system. It is noteworthy that the RBD expressed in the system does not have any posttranslational modifications near the receptor-binding region. While this method is a proof-of-concept with room for optimization and improvement, it is simple, rapid, and less expensive than expression from eukaryotic or mammalian cells and provides a means to quickly produce protein antigen as the SARS-CoV-2 virus continues to mutate into variants.

The RBD was shown to be active in binding ACE2, albeit at a lower affinity (19.01 nM) than a control RBD (3.87 nM) that was made in insect cells. This lower affinity may be accounted for by the lack of glycosylation at Asn331 and Asn343 and the inclusion of the MBP fusion. The flexibility and length of the linker could allow the MBP to get close to the RBM. The RBD-MBP fusion protein performed well in the Luminex immunoassay. We found that the solubility of MBP made the fusion protein easy to work, but it was interesting how effective the MBP fusion was in our serological immunoassay. We think that this is because it has a relatively high lysine content (10%) relative to the RBD (5%) increasing the likelihood that the MBP is crosslinked to the Luminex beads instead of the RBD, thus increasing antigen presentation. We are currently investigating whether or not this hypothesis is correct.

4 | MATERIALS AND METHODS

4.1 | Protein expression and purification

The genetic sequence of spike RBD was fused to ×10-His-tagged maltose-binding protein (MBP), cloned into pET28a, and ordered from GenScript (Figure 2b) with codon-optimization for expression in *E. coli*. To ensure that all five disulfide bonds in the RBD (Figure 1)[4] remain oxidized when expressed in the highly reducing cytoplasm of *E. coli*, we co-expressed the RBD-MBP fusion protein with a CyDisCo plasmid.[24] The plasmids were co-expressed in one-shot BL21(DE3) cells (Thermofisher) in Luria-Bertani media (Fisher Bioreagents) under kanamycin (30 μg/ml) and chloramphenicol (34 μg/ml) selection. Cells were grown at 30°C, 275 rpm shaking until an OD_{600} of 0.3–0.4 was reached, and then induced with a final concentration of 0.5 mM isopropyl β-D-1-thiogalactopyranoside (IPTG) (Gold Biotechnology). At this point, the cells were cooled and transferred to 18°C, 150 rpm shaking overnight (∼16 h; Figure 3). Cells were pelleted at OD600 of 0.8–1.0 and stored at −20°C.

A cell pellet was thawed and resuspended in a buffer containing 20 mM Tris–HCl pH 7.4, 0.2 M NaCl, and 50 μl of protease inhibitor cocktail (Sigma, Cat.# P8849) per gram of cell pellet. The resuspended pellet was then lysed by three passes through an Emulsiflex C3. The resulting lysate was clarified by centrifugation at

40,000 × *g* for 30 min at 4°C. Clarified lysate was then filtered through a 0.45 μm filter (Millipore) before being passed through a 5 ml MBPTrap column (GE) using an AKTA FPLC (Amersham Biosciences, UK). Nonspecifically bound proteins were washed from the column with 10 CV of resuspension buffer, and RBD-MBP was eluted over 10 CV in a gradient method, using a buffer containing 20 mM Tris–HCl pH 7.4, 0.2 M NaCl, and 10 mM maltose. Fractions yielding protein (as observed by A_{280} peaks on the AKTA FPLC (Amersham Biosciences, UK) chromatogram) were gel-verified using a 10% SDS-PAGE gel (Genscript) that was stained with Coomassie Brilliant Blue G-250 for size (Figure 4b), then loaded onto a 1 ml NiAff column (GE) with a running buffer containing ×2 PBS with 20 mM imidazole, pH 8, and an elution buffer containing ×2 PBS with 1 M imidazole, pH 8 over 16 CV. The use of two affinity chromatography steps significantly reduced the number of nonspecific bands resulting from using either just the MBP-tag or the His-tag for purification and also helped eliminate most of the endogenous and recombinant MBP which can be seen in Figure 4b. The resulting peaks were again gel-verified (Figure 4c), and lanes with bands corresponding to 74 kDa (expected size of the RBD-MBP fusion protein) were concentrated and loaded onto a HiLoad 16/60 Superdex75 (GE) size-exclusion column. Fractions corresponding to the fusion protein (Figure 4d,e), were pooled and concentrated (using Amicon regenerated cellulose concentrators (Cat # UFC803096). RBD-MBP identity after each column was confirmed by Peggy Sue (Protein Simple) western analysis using Sino Biological Anti-Coronavirus spike antibody (Cat # 40591-T62). The concentrations were determined using a Fisher NanoDrop1000 using a molecular weight of 74 kDa for the fusion protein and calculated $\epsilon_{280} = 101{,}190\ M^{-1}\ cm^{-1}$. Purified RBD-MBP was stored at −20°C in ×2 PBS supplemented with a final concentration of 30% glycerol.

4.2 | Surface plasmon resonance (SPR) based hACE2 binding assay

The recombinant hACE2-AviTag protein from 293 T cells (Acro Biosystems, DE) was captured on a sensor chip in the test flow channels. As a positive control we used SARS-CoV-2 (2019-nCoV) Spike RBD-His Recombinant Protein (Sinobiological Cat No. 40592-V08B) including residues Arg319-Phe541 expressed in insect cells with a polyhistidine tag at the C-terminus. Samples of 300 μl of freshly prepared serial dilutions of the purified recombinant protein were injected at a flow rate of 50 μl/min (contact duration 180 s) for the association. Responses from the protein surface were corrected for the response from a mock surface and responses from a buffer-only injection. Total hACE2 binding and data analysis were calculated with Bio-Rad ProteOn Manager software (version 3.1).

4.3 | Luminex serological assay

This assay was performed using the purified SARS-CoV-2 RBD-MBP fusion (5 μg per 106 beads) coupled to the surface of group A, region 43, MagPlex Microspheres (Luminex Corp, IL). Microsphere coupling was performed using the Luminex xMAP Antibody Coupling Kit (Luminex Corp, IL) according to the manufacturer's instructions. The protein-coupled microspheres were re-suspended in PBS-TBN buffer (×1 PBS containing 0.1% Tween 20, 0.5% BSA and 0.1% sodium azide) at a final stock concentration of 2×10^6 microspheres per ml, with 2.5×10^3 microspheres used per reaction. De-identified serum samples were obtained from residual patient sera that tested positive or negative by a clinical SARS-CoV-2 serology assay (Diasorin LIASON SARS-CoV-2 S1/S1 IgG; $n = 6$ per group) at UNMC. Fifty microliter of each serum sample (diluted 1:50 with ×1 PBS-TBN buffer) was mixed with 50 μl of the RBD-MBP coupled microspheres in a 96-well plate. The assay plate was incubated for 30 min at 37°C with shaking at 700 rpm and then washed five times with ×1 PBS-TBN buffer. Then, the plate was incubated with biotin-conjugated goat anti-human IgG (Abcam, MA), labeled with streptavidin R-phycoerythrin reporter (Luminex xTAG SA-PE G75) for 1 h at 25°C with shaking at 700 rpm. Then, the plate was washed five times with ×1 PBS-TBN buffer. Finally, the plate was re-suspended in 100 ml of ×1 PBS-TBN buffer and incubated for 10 min at 25°C with shaking at 700 rpm. The microplate was assayed on a Luminex MAGPIXTM System, and results were reported as median fluorescent intensity (MFI).

ACKNOWLEDGMENTS

The authors thank Dr. Lloyd Ruddock at the Oulun Yliopisto, Oulu, Finland for kindly gifting the CyDisCo plasmid and providing essential advice on its use for this study. This research was supported by the Fred and Pamela Buffett NCI Cancer Center Support Grant (P30CA036727) and its associated COVID19 supplement.

CONFLICT OF INTEREST

The authors declare no conflicts of interest.

AUTHOR CONTRIBUTIONS

Janani Prahlad: Investigation; methodology; writing-original draft; writing-review & editing. **Lucas Struble:** Investigation; methodology; writing-review & editing.

William Lutz: Investigation; methodology; writing-review & editing. **Savanna Wallin:** Investigation; methodology; writing-review & editing. **Surender Khurana:** Methodology; writing-review & editing. **Andrew Schnaubelt:** Methodology; writing-review & editing. **Mara Broadhurst:** Methodology; writing-review & editing. **Kenneth Bayles:** Funding acquisition; writing-review & editing. **Gloria Borgstahl:** Conceptualization; funding acquisition; supervision; visualization; writing-original draft; writing-review & editing.

ORCID

Gloria E. O. Borgstahl https://orcid.org/0000-0001-8070-0258

REFERENCES

1. Zhang R, Li Y, Zhang AL, Wang Y, Molina MJ. Identifying airborne transmission as the dominant route for the spread of COVID-19. Proc Natl Acad Sci U S A. 2020;117:14857–14863.
2. Andersen KG, Rambaut A, Lipkin WI, Holmes EC, Garry RF. The proximal origin of SARS-CoV-2. Nat Med. 2020;26:450–452.
3. Mehdipour AR, Hummer G. Dual nature of human ACE2 glycosylation in binding to SARS-CoV-2 spike. Proc Natl Acad Sci U S A. 2021;118:e2100425118.
4. Lan J, Ge J, Yu J, et al. Structure of the SARS-CoV-2 spike receptor-binding domain bound to the ACE2 receptor. Nature. 2020;581:215–220.
5. Wrapp D, Wang N, Corbett KS, et al. Cryo-EM structure of the 2019-nCoV spike in the prefusion conformation. Science. 2020;367:1260–1263.
6. Tai W, He L, Zhang X, et al. Characterization of the receptor-binding domain (RBD) of 2019 novel coronavirus: Implication for development of RBD protein as a viral attachment inhibitor and vaccine. Cell Mol Immunol. 2020;17:613–620.
7. Huang Y, Yang C, Xu XF, Xu W, Liu SW. Structural and functional properties of SARS-CoV-2 spike protein: Potential antivirus drug development for COVID-19. Acta Pharmacol Sin. 2020;41:1141–1149.
8. McCallum M, Walls AC, Bowen JE, Corti D, Veesler D. Structure-guided covalent stabilization of coronavirus spike glycoprotein trimers in the closed conformation. Nat Struct Mol Biol. 2020;27:942–949.
9. Rossi GA, Sacco O, Mancino E, Cristiani L, Midulla F. Differences and similarities between SARS-CoV and SARS-CoV-2: Spike receptor-binding domain recognition and host cell infection with support of cellular serine proteases. Infection. 2020;48:665–669.
10. Walls AC, Park YJ, Tortorici MA, Wall A, McGuire AT, Veesler D. Structure, function, and antigenicity of the SARS-CoV-2 spike glycoprotein. Cell. 2020;183:1735.
11. Zhu G, Zhu C, Zhu Y, Sun F. Minireview of progress in the structural study of SARS-CoV-2 proteins. Curr Res Microb Sci. 2020;1:53–61.
12. Shang J, Ye G, Shi K, et al. Structural basis of receptor recognition by SARS-CoV-2. Nature. 2020;581:221–224.
13. Wang Q, Zhang Y, Wu L, et al. Structural and functional basis of SARS-CoV-2 entry by using human ACE2. Cell. 2020;181:894–904.
14. Roy A, Kucukural A, Zhang Y. I-TASSER: A unified platform for automated protein structure and function prediction. Nat Protoc. 2010;5:725–738.
15. Yang J, Yan R, Roy A, Xu D, Poisson J, Zhang Y. The I-TASSER suite: Protein structure and function prediction. Nat Methods. 2015;12:7–8.
16. Zhang Y. I-TASSER server for protein 3D structure prediction. BMC Bioinformatics. 2008;9:40. https://bmcbioinformatics.biomedcentral.com/articles/10.1186/1471-2105-9-40.
17. Watanabe Y, Allen JD, Wrapp D, McLellan JS, Crispin M. Site-specific glycan analysis of the SARS-CoV-2 spike. Science. 2020;369:330–333.
18. Allen JD, Watanabe Y, Chawla H, Newby ML, Crispin M. Subtle influence of ACE2 glycan processing on SARS-CoV-2 recognition. J Mol Biol. 2021;433:166762.
19. Zhao P, Praissman JL, Grant OC, et al. Virus-receptor interactions of glycosylated SARS-CoV-2 spike and human ACE2 receptor. Cell Host Microbe. 2020;28:586–601.
20. Henderson R, Edwards, RJ, Mansouri, K et al. Glycans on the SARS-CoV-2 spike control the receptor binding domain conformation. bioRxiv. 2020. https://doi.org/10.1101/2020.06.26.173765.
21. Yang Q, Hughes TA, Kelkar A, et al. Inhibition of SARS-CoV-2 viral entry upon blocking N- and O-glycan elaboration. Elife. 2020;9:e61552.
22. Zhang Y, Zhao, W, Mao, Y et al. Site-specific N-glycosylation characterization of recombinant SARS-CoV-2 spike proteins. Mol Cell Proteomics. 2021;20:100058. https://doi.org/10.1101/2020.03.28.013276.
23. Pettersen EF, Goddard TD, Huang CC, et al. UCSF Chimera: A visualization system for exploratory research and analysis. J Comput Chem. 2004;25:1605–1612.
24. Gaciarz A, Khatri, NM, Velez-Suberbie, ML et al. Efficient soluble expression of disulfide bonded proteins in the cytoplasm of *Escherichia coli* in fed-batch fermentations on chemically defined minimal media. Microb Cell Fact. 2017;16:108.
25. Nguyen VD, Hatahet F, Salo KES, Enlund E, Zhang C, Ruddock, LW. Pre-expression of a sulfhydryl oxidase significantly increases the yields of eukaryotic disulfide bond containing proteins expressed in the cytoplasm of *E. coli*. Microb Cell Fact. 2011;10:1.
26. Berkmen M. Production of disulfide-bonded proteins in *Escherichia coli*. Protein Expr Purif. 2012;82:240–251.
27. Hatahet F, Nguyen VD, Salo KEH, Ruddock LW. Disruption of reducing pathways is not essential for efficient disulfide bond formation in the cytoplasm of *E. coli*. Microb Cell Fact. 2010;9:67.
28. Hatahet F, Ruddock LW. Protein disulfide isomerase: A critical evaluation of its function in disulfide bond formation. Antioxid Redox Signal. 2009;11:2807–2850.

How to cite this article: Prahlad J, Struble LR, Lutz WE, Wallin SA, Khurana S, Schnaubelt A, et al. CyDisCo production of functional recombinant SARS-CoV-2 spike receptor binding domain. Protein Science. 2021;1–8. https://doi.org/10.1002/pro.4152